Journal of Crohn's and Colitis, 2022, 286–300
https://doi.org/10.1093/ecco-jcc/jjab129
Advance Access publication July 21, 2021
Original Article

Original Article

Therapeutic siRNAs Targeting the JAK/STAT Signalling Pathway in Inflammatory Bowel Diseases

Flora Clément,[a,b,*] Adrien Nougarède,[c] Stéphanie Combe,[a] Frédérique Kermarrec,[a] Arindam K. Dey,[b] Patricia Obeid,[a] Arnaud Millet,[d] Fabrice P. Navarro,[c] Patrice N. Marche,[b] Eric Sulpice,[a,*] Xavier Gidrol[a,*]

[a]Univ. Grenoble Alpes, CEA, INSERM, IRIG, Biomics, F-38000, Grenoble, France [b]Univ. Grenoble Alpes, INSERM U1209, CNRS UMR5309, IAB, F-38700, La Tronche, France [c]Univ. Grenoble Alpes, CEA, Leti, Division for Biology and Healthcare Technologies, Microfluidic Systems and Bioengineering Lab, F-38000, Grenoble, France [d]Univ. Grenoble Alpes, Inserm U1209, CNRS UMR5309, Team Mechanobiology, immunity and Cancer, Institute for Advanced Biosciences, F-38700, La Tronche, France

*These authors contributed equally to this work.

Corresponding author: Xavier Gidrol, Univ. Grenoble Alpes, CEA, INSERM, IRIG, Biomics, F-38000, Grenoble, France. Tel: +(33)4 38 78 22 36; Fax: +(33)4 38 78 59 17; Email: xavier.gidrol@cea.fr

Abstract

Background and Aims: Inflammatory bowel diseases are highly debilitating conditions that require constant monitoring and life-long medication. Current treatments are focused on systemic administration of immunomodulatory drugs, but they have a broad range of undesirable side-effects. RNA interference is a highly specific endogenous mechanism that regulates the expression of the gene at the transcript level, which can be repurposed using exogenous short interfering RNA [siRNA] to repress expression of the target gene. While siRNA therapeutics can offer an alternative to existing therapies, with a high specificity critical for chronically administrated drugs, evidence of their potency compared to chemical kinase inhibitors used in clinics is still lacking in alleviating an adverse inflammatory response.

Methods: We provide a framework to select highly specific siRNA, with a focus on two kinases strongly involved in pro-inflammatory diseases, namely JAK1 and JAK3. Using western-blot, real-time quantitative PCR and large-scale analysis, we assessed the specificity profile of these siRNA drugs and compared their efficacy to the most recent and promising kinase inhibitors for Janus kinases [Jakinibs], tofacitinib and filgotinib.

Results: siRNA drugs can reach higher efficiency and selectivity at lower doses [5 pM *vs* 1 μM] than Jakinibs. Moreover, JAK silencing lasted up to 11 days, even with 6 h pulse transfection.

Conclusions: The siRNA-based drugs developed hold the potential to develop more potent therapeutics for chronic inflammatory diseases.

Graphical Abstract

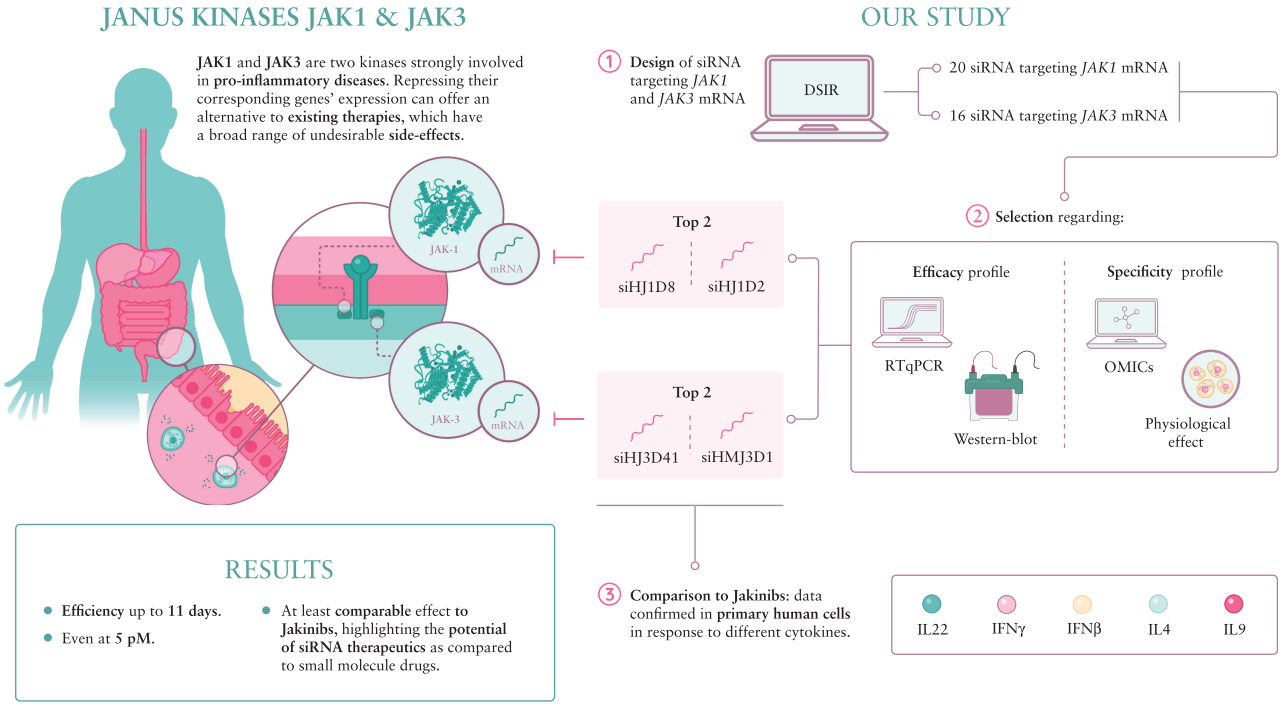

Key Words: Therapeutic siRNA; JAK inhibitors; inflammatory bowel diseases

1. Introduction

The Janus kinase/signal transducers and activators of transcription [JAK/STAT] proteins are key effectors of inflammation that recently have been gaining increasing attention in clinics. This pathway plays a central role in integrating cell signalling cues and coordinating the inflammatory response within immune cells, and it is involved in numerous inflammatory disorders, ranging from chronic inflammatory disorders such as Crohn's disease, ulcerative colitis, polyarthritis rheumatoid or dermatological diseases to the dramatic cytokine burst recently highlighted in COVID-19 patients.[1–3] The JAK family is composed of four different protein kinase members, namely JAK1, JAK2, JAK3 and TYK2. They play a major role in the signal transduction pathways triggered by cytokines such as interleukins and interferons. Indeed, receptor activation leads to JAK recruitment and phosphorylation. JAKs can form homo- or heterodimers, which, in turn, activate and phosphorylate STATs, allowing their translocation to the nucleus where they bind to DNA-specific response elements and act as transcription factors. Depending on the ligand, mainly cytokines such as interleukin [IL] and interferon [IFN] but also growth factors such as insulin-like growth factor-1, the composition of JAK dimers leads to several distinct cell responses through various STAT activation cascades.[4,5] Since JAKs are key effectors in inflammation, targeting Janus kinases remains a critical issue in these pathologies. Immense efforts have been dedicated to the development of specific JAK inhibitors [Jakinibs] that target its kinase activity.[6] Among the Jakinibs, two have been particularly studied and evaluated in clinical trials for inflammatory bowel disease: tofacitinib and filgotinib. For instance, tofacitinib has already been approved for the treatment of rheumatoid arthritis, psoriatic arthritis, juvenile idiopathic arthritis and ulcerative colitis,[7,8] while filgotinib, recently approved for rheumatoid arthritis, is under evaluation for both ulcerative colitis and Crohn's disease in the FITZROY cohort.[7,9,10] However, the newly designed drugs are not yet fully satisfactory in terms of specificity, adverse events and side effects such as risks of infection including herpes zoster.[11–13]

To avoid systemic delivery and enhance selectivity, we designed highly specific JAK1 or JAK3 inhibitors based on short interfering RNA [siRNA], leading to the knockdown of JAK1 and JAK3 expression by targeting their mRNA. RNA interference [RNAi] was highlighted by Craig Mello and Andrew Fire in 1998, and they were awarded the Nobel Prize in Physiology and Medicine in 2006 for their research work. RNAi involves short double-stranded ribonucleic acids that interfere through sequence-specific recognition and pairing with a specific mRNA and leads to its degradation or prevents its translation, inducing the knockdown of the corresponding protein.[14] This mechanism is naturally present in cells and allows the micro-RNA (miRNA) to regulate mRNA and protein expression. It can also be induced by synthetic short hairpin RNA [shRNA] and siRNA. Unlike gene therapy, which is based on modification of the genome within the nucleus, siRNAs act directly in the cell cytoplasm through the RISC multiprotein complex and require neither nuclear import nor integration into the genome.[15] Therefore, siRNA therapies avoid the threat of introducing cancer-leading mutations into the genome of patients. Indeed, due to the benefits of siRNA drugs, patisiran and givlaari were recently approved for the treatment of hereditary transthyretin amyloidosis and acute hepatic porphyria, respectively.[16,17] These studies highlight the therapeutic potential of siRNAs in treating liver diseases. We now wish to extend these

innovative solutions to other tissues such as the intestinal tract to cure inflammatory bowel diseases. While RNAi gave some concerns relative to potential off-target effects,[18] we sought to demonstrate that siRNAs possess a better efficiency at a lower dose and specificity profile by providing a side-by-side comparison with the chemical Jakinibs, tofacitinib and filgotinib. In this study, we identified two highly selective JAK1 and JAK3 siRNA sequences. We analysed their effects on human cells [both primary immune cells and cell lines including colonic epithelial cells], providing an exhaustive study of both the efficacy and specificity profile of the sequences relative to the currently available chemical kinase inhibitors.

2. Methods

2.1. Cell culture

2.1.1. Cell lines

CACO-2 [human epithelial colorectal adenocarcinoma cells; #HTB-37], PC3 [human epithelial prostate cancer cells, #CRL-1435] and T47D [human epithelial breast cancer cells; #HTB-133] cell lines were obtained from the ATCC and maintained at 37°C in 5% CO_2, according to the manufacturer's recommendations. CACO-2 and T47D cells were grown in Dulbecco's modified Eagle medium [DMEM] 4.5 g/L glucose containing GlutaMAX and pyruvate [ThermoFisher Scientific cat. #31966-021] and in Roswell Park Memorial Institute 1640 [RPMI 1640] medium GlutaMAX [ThermoFisher cat. #61870044] for PC3 cells. All cell culture media were supplemented with 10% fetal bovine serum [Premium South America Dominique Dutscher cat. #P30-3302C lot P150205] and 100 U/mL penicillin and 100 µg/mL streptomycin [Life Technologies cat. #15140-122]. All cell lines were routinely tested for mycoplasma contamination.

2.1.2. Primary human macrophages

These were prepared according to the protocol established by Court and colleagues.[19] Human blood samples from healthy de-identified donors were obtained from EFS [French national blood service] as part of an authorized protocol [CODECOH DC-2015-2502]. Donors gave signed consent for their blood to be used in this exploratory study. Briefly, primary peripheral blood mononuclear cells [PBMCs] were sorted using CD14 magnetic beads, then differentiated into unpolarized macrophages for 6 days in RPMI glutamax [Life Technologies cat. #61870044] supplemented with 10 mM HEPES [Life Technologies cat. #15630-080], non-essential amino acids [NEAA] [Life Technologies cat. #11140-035], 10% human serum [AB plasma cat. #H4522], 25 ng/mL macrophage colony stimulating factor [M-CSF]; subsequently, 1 ng/mL lipopolysaccharide [LPS] stimulation for 6 h was performed to polarize cells into pro-inflammatory macrophages.

2.1.3. JAK1 and JAK3 overexpressing cells

PC3 cells were transfected with the plasmid pcDNA3.1-HsJAK3-C-eGFP [GenScript; clone ID OHu18003C; NM_000215.4] to trigger ectopic overexpression of JAK3 fused to the green fluorescent protein [GFP]. Cells with stable expression for fusion proteins were selected by G418 at 600 µg/mL for at least five passages, and clones were then sorted using the cell cytometer MELODY (Becton Dickinson) and the Chorus software.

2.2. siRNA design and primary selection

siRNA sequences were designed to target JAK1 [NM_00227] and JAK3 [NM_000215] mRNA using the Designer of Small Interfering RNA [DSIR] algorithm.[20] The DSIR includes specific tools and algorithms that help prevent off-target effects such as the following: [i] the guide strand of our siRNAs possesses a perfect match for the mRNA target only; [ii] known pro-inflammatory-stimulating motif such as toll-like receptor [TLR] motifs are automatically removed during the design; [iii] specific 3′ and 5′ GC and AU content have been applied to favour the guide strand in place of passenger strand processing by the RISC, all criteria being critical for avoiding siRNA off-targeting.[21,22] The DSIR also gives information on putative sequence homology between the seed region of the guide strand and the 3′-UTR mRNA of the whole genome. Indeed, siRNAs have been described for their potential off-target gene regulation through an miRNA-like mechanism.[23–25] The greater number of seed sequence homology on the same 3′-UTR, the higher the risk of having miRNA-like effects. During siRNA synthesis, the guide strand has been chemically modified with the addition of a 5′-P to favour guide strand processing by RISC. The siRNA sequences were designed with 21 nucleotides. The seed complement frequencies using seed length were set at 7 nucleotides with a mismatch tolerance of 1. Based on the DSIR algorithm, 20 sequences were selected for targeting human *JAK1* [siHJ1D#], while 16 were selected for human *JAK3* [siHJ3D#].

2.3. siRNA transfection

For siRNA transfection, lipofectamine RNAiMAX [Invitrogen cat. #13778-150] and Opti-MEM medium [Gibco cat. #11058-021] were used. CACO-2 cells were reverse transfected using 10^5 cells per well seeded on a 12-well plate, except for transcriptomic analysis, where 10^6 CACO-2 cells were seeded in 10-cm-diameter dishes. For T47D and PC3 cells, 7×10^4 to 8×10^4 cells were seeded per well on a 12-well plate 24 h before the transfection. The transfection was performed using 0.8 µL [CACO-2] or 1 µL [PC3 and T47D] of lipofectamine RNAiMAX per well and mixed with the siRNA at different concentrations, according to the manufacturer's instructions. For primary immune cells, the transfection was performed using lipofectamine RNAiMAX by means of a 6-h pulse in Opti-MEM media, and the media were then changed into complete media. Cells were harvested 48 h after the transfection, unless otherwise specified, for downstream experiments.

2.4. Apoptosis analysis

Cell apoptosis was monitored by a Becton Dickinson LSR2 flow cytometer and Diva 6.0 software using the CellEvent Caspase-3/7 green detection reagent [Thermo Fischer Scientific, cat. #C10423], according to the manufacturer's instructions. Briefly, CellEvent reagent was added at 2 µM 72 h after cell transfection. Cells were then harvested and fixed in 4% paraformaldehyde (PFA) in PBS before fluorescence-activated cell sorting (FACS) analysis. The siRNA inducing cell apoptosis [Qiagen; Hs Cell-Death control siRNA] was used as a positive control.

2.5. Cell proliferation analysis

Cell proliferation was analysed using flow cytometry following EdU incorporation during the S phase with the Click-It EdU Alexa Fluor 647 Flow cytometry assay [Thermo Fischer Scientific, cat. #C10419], as per the manufacturer's instructions. Briefly, a total of 5 µM EdU was added to the culture medium on the 3rd day of transfection, for 5 h, before harvesting the cells and proceeding to cell fixation in 4% PFA and FACS analysis. An siRNA targeting the kinesin-related molecular motor EG5 [Qiagen Hs siKIFF11_6] was used as a positive

control, with its transfection inducing mitotic arrest and then cell apoptosis.

2.6. Metabolism analysis

ATP levels reflecting cell metabolism correlated with cell proliferation and viability were analysed using the ViaLight Plus Cell Proliferation and Cytotoxicity Bioassay kit [Lonza, #LT07-121], according to the manufacturer's instructions. Briefly, 3000 CACO-2 cells were seeded into 96-well plates. Three days after the transfection, 25 µL per well of Cell Lysis Reagent was added to the cells, then the ATP level was quantified using 50 µL AMR PLUS reagent with a GloMax luminometer. The Hs Cell-Death control siRNA was used as a positive control of cell transfection.

2.7. High content screening

PC3 clones overexpressing JAK3 fused to GFP were seeded into 96 black µClear cell culture well plates in antibiotic-free RPMI medium containing 10% fetal bovine serum. After 24 h of culture, cells were transfected with different siRNA sequences targeting *JAK3* using the lipofectamine RNAiMAX transfection agent, according to the manufacturer's instructions. The non-targeting siRNA siAllStars [AllStars negative control siRNA, referred to as siMock] and an siRNA targeting the *GFP* [siGFP-22 from Qiagen] gene were used as negative and positive controls, respectively. After 48 h of transfection, cells were fixed with 2% PFA for 15 min, and cell nuclei were then stained using 5 µM Hoechst 33342 for 10 min. After two washes with PBS, the wells were filled with 100 µL PBS containing 50% glycerol. Plates were stored at 4°C in the dark before analysis. GFP quantification was performed at a single-cell level using a CellInsight NXT automated microscope using 10× objectives and HCS Studio. The siRNA sequences were tested in triplicate at concentrations of 10 and 1 nM. Cell fluorescence levels were extracted after cell segmentations on ten different fields per well, and data were analysed at the cellular level using the R software.

2.8. Toll-like receptor [TLR] activation monitoring

The stimulation of TLR receptors [TLR1/2/3/4/5/9] was monitored using THP1-XBlue-MD2-CD14 cells [Invivogen cat. #thpx-mdcdsp], a human monocytic cell line engineered to stably express NF-κB and the AP-1-inducible secreted embryonic alkaline phosphatase [SEAP] reporter gene. This cell line stably expresses all TLRs and a reporter gene allowing TLR activation through absorbance of the culture medium. As controls, 10^7 cells were incubated with 1 ng/mL Pam3CSK4, 10^7 cells/mL HKLM, 10 µg/mL poly[I:C], 10 ng/mL LPS-EK, 10 ng/mL RecFLA-ST or 10 µg/mL CpG ODN2006 to respectively activate TLR1/2, TLR2, TLR3, TLR4, TLR5 or TLR9. After 24 h of incubation, culture supernatants were incubated with QUANTI-Blue solution [Invivogen cat. #rep-qbs] for 1 h, then SEAP activity was measured by reading the absorbance at 655 nm with a CLARIOstar Microplate Reader [BMG LABTECH].

2.9. Gene expression analysis

RNA was extracted using RNeasy Plus Mini Kits [Qiagen cat. #74136/74134]. The RNA concentration was measured using a Nanodrop ND-1000 spectrophotometer. Reverse transcription was conducted on 500 ng RNA using a Superscript Vilo cDNA synthesis kit [Invitrogen cat. #11754-050] following the manufacturer's instructions. cDNA was kept at –20°C for further analysis. Quantitative PCR [qPCR] was performed using sequence-specific primers [detailed in Table 1] on a CFX Connect real-time PCR [Bio-Rad] with Platinum SYBR Green qPCR SuperMix-UDG [Invitrogen cat. #11733-046]. GAPDH was used as the reference gene. To conduct RNASeq analysis, RNA contents of CACO-2 cells transfected for 2 days with 100 pM of siRNA using lipofectamine RNAiMAX or incubated for 2 days with 1 µM tofacitinib or 5 µM filgotinib were analysed by the IPMC platform. Negative controls included cells cultivated in a cell medium, in a cell medium with DMSO, exposed to lipofectamine RNAiMAX, or transfected with a mock siRNA. RNASeq data sets were deposited in the ArrayExpress database [fgsubs #491636].

Table 1. RT-qPCR primers

Target	Role	Catalogue number
JAK1	JAK family	Hs_JAK1_1_SG #QT00050225
JAK2		Hs_JAK2_1_SG #QT00062650
JAK3		Hs_JAK3_1_SG #QT00078673
TYK2		Hs_TYK2_1_SG #QT00012978
GAPDH	Housekeeping gene	Hs_GAPDH_1_SG #QT00079247
FECH	From blast of siHJ1D2	Hs_FECH_1_SG #QT00069496
TAF4		Hs_TAF4_1_SG #QT00074179
ABLIM1		Hs_ABLIM1 #QT00057015
ZFYVE1		Hs_ZFYVE1_va.1_SG #QT01021013
ARL14EP		Hs_ARL14EP_1_SG #QT00079660
ZNF782	From blast of siHJ1D8	Hs_ZNF782_1_SG #QT01032087
CADPS2		Hs_CADPS2_1_SG #QT00021497
OAS1		Hs_OAS1 #QT00099134
ZDHHC23		Hs_ZDHHC23 #QT00006125
ZSWIM4		Hs_ZSWIM4_1_SG #QT00077672
LRCH2	From blast of siHJ3D41	Hs_LRCH2_1_SG #QT00011816
RNPEP		Hs_RNPEP #QT00073493
PHF21A		Hs_PHF21A #QT00082215
FAM213A		Hs_FAM213A_2_SG #QT00077119
KANK3	From blast of siHMJ3D1	Hs_KANK3 #QT00218498
TMEM120B		Hs_TMEM120B #QT01193122
POLDIP3		Hs_POLDIP3 #QT00072289
IRF9	Target genes of JAK/STAT pathway	Hs_IRF9_1_SG #QT00001113
DGUOK		Hs_DGUOK_1_SG #QT00066549

2.10. Western-blot analysis

Cell lysis was performed using RIPA lysis buffer [SIGMA cat. #R0278], complemented with a protease inhibitor cocktail [Alpha complete Roche cat. #04 693 124 001]. For phosphorylation analysis, RIPA buffer was also supplemented with 100 mM sodium orthovanadate [Sigma cat. #S6508], 20 g/L sodium fluoride [Sigma cat. #919] and 800 mM β-glycerophosphate [Sigma cat. #G5422]. The BCA assay was used to quantify and normalize loading protein quantities. A total of 10 µg of protein per sample was mixed with Novex NuPAGE LDS Sample Buffer 4× [Thermofisher cat. #NP0007] and Novex NuPAGE Reducing agent 10× [Thermofisher cat. #NP0004] and heated for 10 min at 90°C before separation on Novex NuPAGE Bis-Tris Mini Gels 4–12% [Thermofisher cat. #NP0322BOX] and transferred on a nitrocellulose membrane [Dominique Dutscher cat. #10600019] for 60 min at 10 V. After

incubation with 5% BSA [Sigma cat. #A9647] in TBS-T 1× [Ozyme #9997S] for 30 min, the membranes were incubated with antibodies, as detailed in Table 2, at 4°C overnight. The membranes were washed three times for 10 min and incubated with a 1:10 000 dilution of peroxidase-conjugated AffiniPure Goat antiMouse or Rabbit IgG [H + L] antibodies in 5% BSA TBS-T [Jackson Immunoresearch mouse cat. #115-035-146 lot 135422, rabbit cat. #111-035-003 lot 104122] for 1 h. The blots were washed with TBS-T 1× three times and developed with the ECL system [Pro: Perkin Elmer cat. #NEL122001EA, Prime: Dominique Dutscher cat. #RPN2232, Femto: ThermoFisher Scientific cat. #34095], as per the manufacturer's protocols, using the ChemiDocTouch Gel Imager [BioRad].

2.11. Proteomic analysis—SOMAmer

Protein lysates of CACO-2 cells transfected for 3 days with 10 nM siRNA using lipofectamine RNAiMAX were analysed by the SomaLogic company. The negative control was lipofectamine RNAiMAX-treated cells. Briefly, using their SomaScan Proteomics platform based on aptamers, 1305 different proteins were quantified. Statistical analysis of statistically and differentially expressed proteins [DEPs] was performed by the AltraBio Company. The first filtering was performed as per the following parameters: adjusted $p < 0.05$, fold-change > ×1.23, or < /1.23. This allowed the comparison of 484 remaining proteins that are considered as differentially expressed between siRNA and lipofectamine RNAiMAX conditions.

2.12. Statistical analyses

Statistical significance was assessed using the paired Student's *t*-test. The exact *p*-value are indicated in figure legends.

2.13. Ethical statement

Human blood samples from healthy de-identified donors were obtained from EFS [French national blood service] as part of an authorized protocol [CODECOH DC-2015-2502]. Donors gave signed consent for their blood to be used in this exploratory study.

Table 2. Antibodies used for western blotting

Antibody targeting	Dilution	Provider	Catalogue number
GAPDH	1:2500	Santa Cruz Biotechnology	SC-25778
JAK1	1:1000	Cell Signaling Technology	#3332, #9175
JAK2	1:1000	Cell Signaling Technology	#3229
JAK3	1:1000	Cell Signaling Technology	#3775, #5481, #8863s
TYK2	1:1000	Cell Signaling Technology	#9312s
P-STAT1	1:1000	Cell Signaling Technology	#9167
P-STAT2	1:1000	Cell Signaling Technology	#88410
P-STAT3	1:2000	Cell Signaling Technology	#9145

3. Results

3.1. Design and screening of siRNAs targeting *JAK1* and *JAK3*

First, we designed siRNA sequences with a high specificity to target human *JAK1* and *JAK3* genes. To that end, we started from the mRNA sequence of both genes and used the siRNA designer software [DSIR] to identify putative siRNA sequences with strong efficacy and absent immunostimulatory motifs.[20,26] Thus, we generated 20 sequences targeting *JAK1* [siHJ1D#] and 16 targeting *JAK3* [siHJ3D#] [Supplementary Figures 1 and 2 show the position of the sequences on the gene in A, and the sequences in B, respectively].

To select the most efficient siRNA sequences among those identified, we performed cell transfection experiments to analyse knockdown efficiencies at both mRNA and protein levels, using RT-qPCR, western blotting, flow cytometry and high-content fluorescence microscopy quantification. We used three cell lines expressing detectable levels of endogenous JAK1 protein: the colon cell line CACO-2, the prostate cell line PC3 and the breast cell line T47D [Supplementary Figure 3A]. However, as these cell lines did not express endogenous JAK3 to a sufficient level to enable knockdown analysis, we engineered PC3 cells to express a JAK3-GFP fusion protein with a high stability level [Supplementary Figure 3B]. The same approaches were used for JAK1 to quantify knockdown efficiency. To filter the top sequences targeting *JAK1* that trigger the highest knockdown efficiency with the lowest off-target effects, we first classified the sequences using *in silico* analysis and information provided by the DSIR, which allowed us to filter the top ten sequences. For instance, siHJ1D4 was selected as it corresponded to the highest corrected score [98.7] despite a putative high 3′ untranslated region [UTR] recognition score [putative miR-like effects] [≥3 hits score], while siHJ1D5/6/9/19/20/33/37/81 were selected on the high ≥3 hits score, and siHJ1D24 was selected on a low corrected score [87.5] [Supplementary Table 1]. The best ten sequences for JAK1 were filtered based on their gene-silencing activity with the help of western-blotting and RT-qPCR after siRNA transfection [Supplementary Table 2]. To obtained the top two siRNAs targeting *JAK1*, we combined the data pertaining to gene-silencing efficiency, the putative 3′UTR hits, and the data obtained from the *in silico* analysis of potential targets of both sense and antisense siRNA sequences using the NCBI blast online platform, a strategy published recently by Mroweh and colleagues[27] [Supplementary Table 3]. Based on this strategy, we further focused on siHJ1D8 and siHJ1D2 sequences in order to target *JAK1* and siHJ3D41 and siHMJ3D1 to then target *JAK3* [Supplementary Tables 4– 6].

3.2. Efficiency of siRNAs targeting *JAK1* and *JAK3*

We then assessed the specificity of the siRNAs selected against other JAK family members. We first transfected mock or *JAK1* and *JAK3* targeting siRNA at 10 nM final concentration in PC3-JAK3-GFP engineered cells before analysing for the protein expression levels of JAK1/2/3 or TYK2 using western blotting to ensure the specificity of our sequences against the JAK protein family. We showed that siHJ1D8 and siHJ1D2 decreased JAK1 protein expression by 96% [Figure 1A], while siHJ3D41 and siHMJ3D1 were able to decrease JAK3 protein expression with a knockdown efficiency of 95% [Figure 1B]. None of these four siRNAs decreased the expression level of JAK2 protein [Figure 1C], whereas a very slight decrease of TYK2 protein expression was observed with siHJ1D8 and siHJ1D2, with knockdown efficiencies of

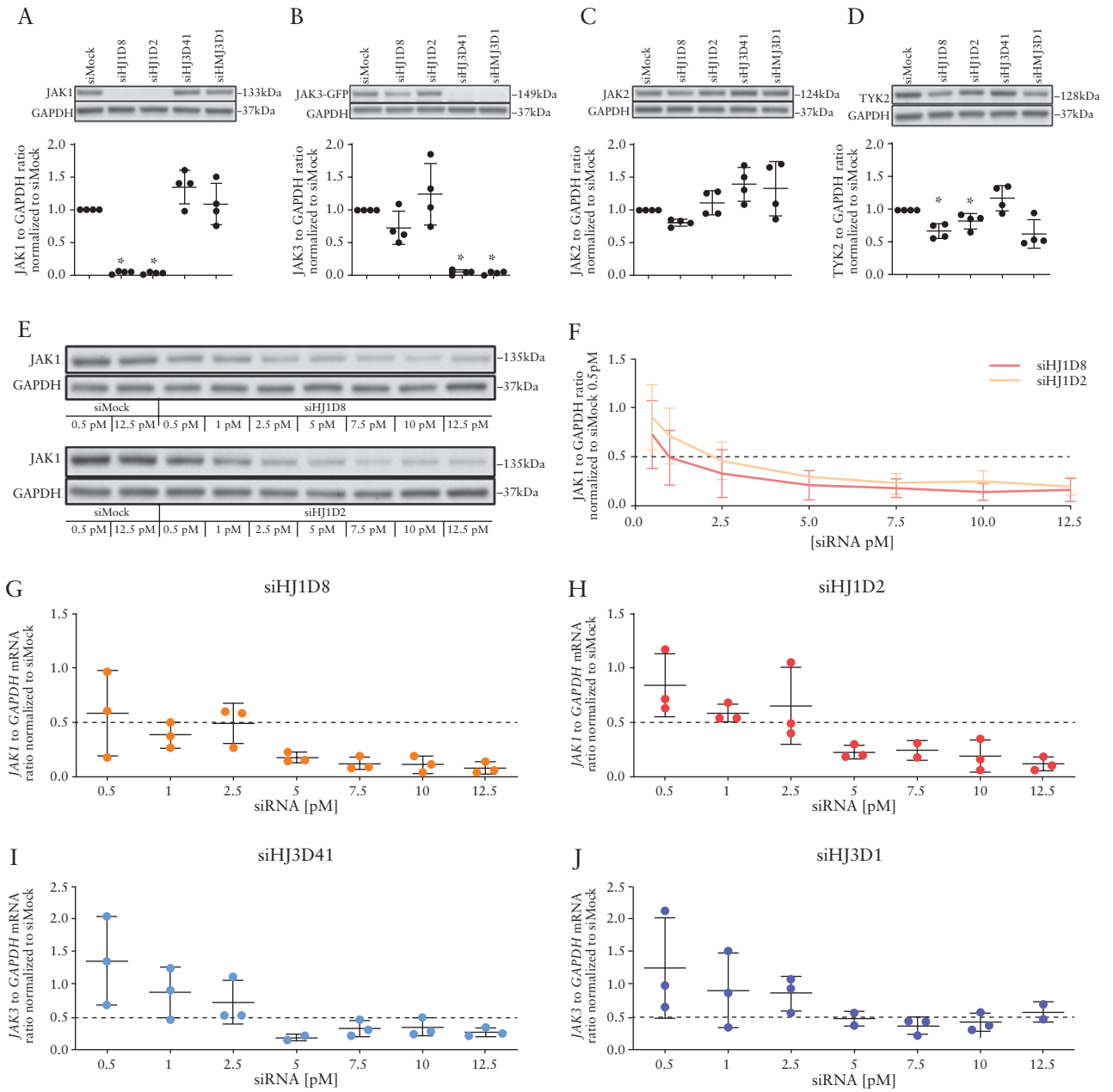

Figure 1. Selectivity and efficiency of *JAK*-targeting siRNAs. Selectivity of the sorted siRNAs was assessed on PC3-JAK3-GFP-engineered cells transfected using lipofectamine RNAiMAX and different siRNAs at 10 nM. Representative western blot analysis is shown on the top panel, with the corresponding quantification at the bottom [$N = 4$ independent experiments] for the expression of JAK1 [A], JAK3 [B], JAK2 [C] or TYK2 [D] proteins. For A, * represents respectively p-values = 0.0307 and 0.0324; for B, * represents respectively p-values = 0.0477 and 0.0456; for D, * represents respectively p-values = 0.0212 and 0.0359. [E] Representative western blot of PC3 cells transfected by *JAK1*-targeting siRNAs at different concentrations ranging from 0.5 to 12.5 pM. [F] Quantification of JAK1 protein expression [$N = 3$ independent experiments] from the experiment shown in **E.** Quantification by RTqPCR of *JAK1* mRNA levels in PC3 cells [G, H] or *JAK3* mRNA levels in PC3-JAK3-GFP-engineered cells [I, J] transfected using lipofectamine RNAiMAX and siRNAs at concentration ranging from 0.5 to 12.5 pM [$N = 3$ independent experiments]. GAPDH was used as a housekeeping gene.

35% and 17%, respectively, as compared to the mock siRNA [Figure 1D]. These results were confirmed in PC3 wild-type cells [Supplementary Figure 3C]. To ensure the physiological relevance of our *JAK*-targeting siRNA sequences in inflammatory disease, we analysed protein expression after siRNA transfection in primary macrophages that were derived from PBMCs. The level of JAK1 protein expression in unpolarized primary macrophages allowed us to study JAK1 downregulation. Both siHJ1D8 and siHJ1D2 were able to efficiently knockdown JAK1 in these cells [Supplementary Figure 3D]. As the level of JAK3 expression was extremely low in these unpolarized cells, we analysed siJAK3 transfection efficiency in pro-inflammatory macrophages, polarized through LPS stimulation. This strategy enabled the detection of JAK3 protein knockdown in human primary immune cells [Supplementary Figure 3E]. The four siRNA-designed sequences can knockdown JAK1 or JAK3 protein expression in primary human macrophages, thereby opening the way for new avenues for the treatment of inflammation-related diseases.

Table 3. Partial sequence homology of siRNA on the genome. Seed sequences [from nucleotide 2 to nucleotide 7] in red and partial homology in bold underlined. * represent gene expressions that were analysed in RTqPCR

siRNA	Gene name	Position on the siRNA sequence	Query cover	Identities	Strand
siHJ1D8	ZFYVE1*	UCGC**UUG**UAGCUGAUGUCCUU	71%	15/15	Sense/Antisense
	ZNF782*	UCGC**UUG**UAGCUGAUGUCCUU	66%	14/14	Sense/Antisense
	TPMT	UCGCUUG**UAGCUGAUGUCCUU**	66%	14/14	Antisense
	OAS1*	UCGCUUG**UAGCUGAUGUCCUU**	66%	14/14	Antisense
	FLO11-like	UCGCU**UG**UAGCUGAUGUCCUU	61%	13/13	Sense/Antisense
	MFSD14B	UCGCU**UG**UAGCUGAUGUCCUU	61%	13/13	Sense/Antisense
	CADPS2*	UCGCU**UG**UAGCUGAUGUCCUU	61%	13/13	Sense/Antisense
	ARL14EP*	**UCGCUUG**UAGCUGAUGUCCUU	61%	13/13	Sense
	MEGF10	UCGCUUG**UAGCUGAUGUCCU**U	61%	13/13	Antisense
	FAM160A1	UCGCUU**G**UAGCUGAUGUCCUU	76%	13/13	Sense/Antisense
	ZDHHC23*	UCGC**UUG**UAGCUGAUGUCCUU	61%	13/13	Sense/Antisense
siHJ1D2	NPBWR2	UU**CGUCA**UCCUUGUAAUCCAU	80%	17/17	Sense/Antisense
	FECH*	UUCG**UCA**UCCUUGUAAUCCAU	71%	15/15	Sense/Antisense
	TAF4*	U**UCGUCA**UCCUUGUAAUCCAU	71%	15/15	Antisense
	ADAMTSL2	**UUCGUCA**UCCUUGUAAUCCAU	66%	14/14	Sense/Antisense
	ABLIM1*	UUCGUC**A**UCCUUGUAAUCCAU	66%	14/14	Antisense
siHJ3D41	ZSWIM4*	UA**CGAUU**UCUGGAAAGUCGCA	76%	16/16	Sense/Antisense
	LRCH2*	U**ACGAUU**UCUGGAAAGUCGCA	71%	15/15	Sense/Antisense
	RNPEP*	UAC**GAUU**UCUGGAAAGUCGCA	66%	14/14	Sense/Antisense
	PHF21A*	UAC**GAUU**UCUGGAAAGUCGCA	66%	14/14	Sense/Antisense
siHMJ3D1	KANK3*	UAG**CGGC**ACAGCUCCACGCUG	71%	15/15	Sense/Antisense
	DNAH9	UAG**CGGC**ACAGCUCCACGCUG	66%	14/14	Sense/Antisense
	FARP1	UAGC**GGC**ACAGCUCCACGCUG	66%	14/14	Sense/Antisense
	TMEM120B*	UAGC**GGC**ACAGCUCCACGCUG	85%	17/18	Antisense
	FAM213A*	UAG**CGGC**ACAGCUCCACGCUG	66%	14/14	Sense/Antisense
	CHD7	UAGC**GGC**ACAGCUCCACGCUG	61%	13/13	Sense/Antisense
	TMEM267	UA**GCGGC**ACAGCUCCACGCUG	61%	13/13	Sense
	MAST4	UAG**CGGC**ACAGCUCCACGCUG	61%	13/13	Sense
	DGKQ	UAG**CGGC**ACAGCUCCACGCUG	61%	13/13	Sense
	GSDMD	UAGCGGCA**CAGCUCCACGCUG**	61%	13/13	Sense/Antisense
	POLDIP3*	U**AGCGGC**ACAGCUCCACGCUG	61%	13/13	Sense/Antisense

As gene silencing was already effective at 10 nM, we further decreased the siRNA concentration to investigate the IC50. To that end, we used a range of siRNA concentrations of 0.5–12.5 pM. Endogenous *JAK1* expression was monitored at both protein and mRNA levels, while *JAK3* was only monitored at mRNA levels due to the weak expression in PC3 cells, close to the protein detection limit. Strikingly, we observed a 50% reduction of JAK1 protein expression using both siHJ1D8 and siHJ1D2 at 2.5 pM [Figure 1E and F]. This result was also observed at the mRNA level for both sequences [Figure 1G and H], thus highlighting the high efficiency and good correlation between mRNA and protein detection for *JAK1*. Regarding *JAK3*, we observed a 50% reduction in mRNA level at 5 pM using both siHJ3D41 and siHMJ3D1 sequences [Figure 1I and J]. Together, our data demonstrate that we identified highly efficient *JAK1*- and *JAK3*-targeting siRNAs.

3.3. Specificity of siRNA targeting *JAK1* and *JAK3*

To verify that these siRNAs were highly specific, we analysed potential off-target effects *in silico* of both sense and antisense siRNA sequences using the NCBI blast online platform. As expected, we did not find any perfect match between the siRNA sequences and the human transcriptome. However, partial homologies were found, as described in Table 3.

We then monitored the mRNA expression using RT-qPCR following siRNA transfection to analyse whether these partial sequence homologies could trigger an alteration in gene expression. Furthermore, although we observed very efficient gene silencing at 10 pM [Figure 1], we choose to work at 10 nM so as to further increase the likelihood of observing potential off-target effects. We decided to analyse genes that displayed partial sequence homology sequences [i] with the siRNA seed sequences, and/or [ii] with at least 13 matches, and [iii] with antisense or both antisense and sense strands. Unfortunately, we could not detect the expression of the

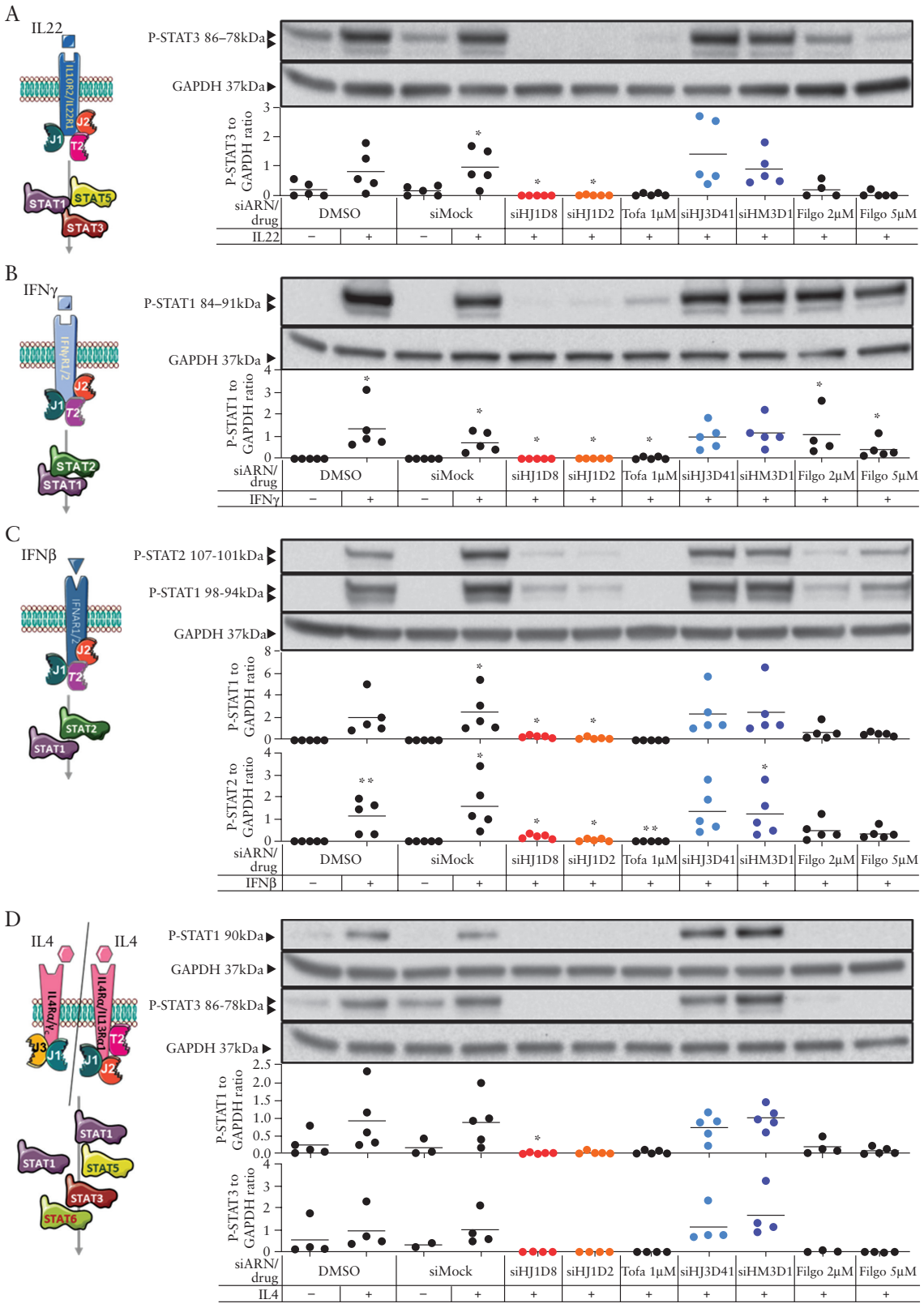

Figure 2. Analysis of sequence-based transcriptomic effects and phenotypic side effects in response to *JAK* modulation. Quantification by RTqPCR of target genes at mRNA levels in T47D cells transfected using lipofectamine RNAiMAX at 10 nM with siHJ1D8 [A], siHJ1D2 [B], siHMJ3D1 [C] or siHJ3D41 [D], dot plot representing $N = 4$ independent experiments. *p*-values: for A: ** = 0.0014; * = 0.0264; for B: ** = 0.0079; for D: ***** = 0.0001, ** = 0.0086. [E] THP1-XBlue-MD2-CD14 cells were treated for 24 h with Pam3CSK4 [1 ng/mL], HKLM [10^7 cells/mL], Poly[I:C] [low/high molecular weight] [10 µg/mL], LPS [10 ng/mL], FLA-ST [10 ng/mL], CpG [10 µg/mL] or siRNAs at final concentration 10 nM. Alkaline phosphatase activity was quantified using a QUANTI Blue Assay, and absorbance was measured at 655 nm and presented as mean ± SD [$N = 6$ independent experiments]. [F] Proliferation analysis in CACO-2 cells, following transfection using

NPBWR2, *ADAMTSL2* and *DNAH9* genes at the mRNA level, either in PC3 or in T47D cell lines. We analysed the effect of the four siRNAs' transfection in T47D cells while *JAK1* or *JAK3* expression levels were monitored as a positive control to ensure transfection efficacy. Among the six genes tested, only *OAS1* showed minor modulation after siHJ1D8 transfection in T47D cells [Figure 2A]. These results were confirmed in PC3 cells, except for *ZDHHC23* and *OAS1* whose expressions were almost undetectable [Supplementary Figure 4A]. After siHJ1D2 transfection, we did not observe any change in expression for the three genes tested in T47D cells [Figure 2B]. Transfection of siHMJ3D1 did not alter the expression of the four genes tested in T47D cells [Figure 2C] nor confirmed the results for one of these candidates in PC3 cells [Supplementary Figure 4B]. Among the three genes tested after siHJ3D41 transfection, a decrease of 85% in *ZSWIM4* mRNA expression level was found on both T47D and PC3 cell lines [Figure 2D and Supplementary Figure 4C]. Moreover, siHJ3D41 transfection in PC3 cells led to a decrease in expression of another gene, *LRCH2* [85%], which was not statistically significant [Supplementary Figure 4C]. In summary, by analysing the different putative off-target effects from the siRNA sequences, we found that siHJ3D41 and siHJ1D8 have more confirmed off-target effects than siHJ1D2 and siHMJ3D1. Therefore, siHJ1D2 and siHMJ3D1 were identified as the most specific siRNAs.

3.4. Phenotypic consequences of the *JAK*s depletion

As the activation of the immune response has been described as a potential off-target effect induced after siRNA transfection, we questioned whether the four sequences were able to activate the innate immune signalling through Toll-like receptors [TLRs].[28] We used the NFkB reporter cell line THP1-XBlue-MD2-CD14 [further referred to as THP1-XBlue cells], derived from the human monocytic THP1 cells. THP1-XBlue cells were exposed to siRNAs at a final concentration of 10 nM. Positive controls such as Pam3CSK4, HKLM, LPS, FLA-ST or CpG were used to confirm TLR activation of TLR1/2, TLR2, TLR4, TLR5 and TLR9, respectively. Neither *JAK1*- nor *JAK3*-targeting siRNA exhibited increased absorbance, indicating that these sequences do not activate the TLR response in immune cells [Figure 2E].

The main phenotypic outcomes were analysed in CACO-2 cells following the transfection of *JAK1* or *JAK3* targeting siRNA, including cell proliferation, apoptotic cell death and cell metabolism. In addition, we used tofacitinib and filgotinib for a direct comparison of the phenotypic effect induced by both siRNA and chemical inhibitors that are used in clinics. The four siRNA sequences had no impact on cell proliferation, apoptosis or metabolism, while filgotinib at 100 µM strongly decreased cell proliferation and ATP levels, and increased apoptosis [Figure 2F–H]. We concluded that the four selected siRNAs had no phenotypic effect on CACO-2 cells, suggesting that, besides their inhibitory efficiency, those *JAK*-targeting siRNAs have minimal impact on the main cell functions, a prerequisite for drug candidates.

3.5. Comparative analysis of *JAK*-targeting siRNAs and effect of chemical inhibitors on JAK/STAT signalling

To analyse the clinical potential of siRNAs to regulate JAK/STAT signalling relative to chemical Jakinibs, filgotinib and tofacitinib, we used western blotting to monitor the activation levels of STAT proteins, the molecular effectors' downstream JAK kinases, using specific phospho-STAT antibodies. We quantified the levels of pro-inflammatory pathways in response to five well-known signalling transduction pathways triggered by IL22, IFNγ, IFNβ, IL4 and IL9 cytokines after siRNA transfection or incubation with Jakinibs. To ensure that siRNAs and both JAK chemical inhibitors were at the right concentrations to block the JAK/STAT signalling cascade, preliminary experiments were conducted in CACO-2 cells, showing that the IL22 signalling pathway was completely blocked using siRNA at 0.2, 1 or 10 nM final concentration [Supplementary Figure 5A–C], or tofacitinib at 1 µM and filgotinib at 5 µM [Supplementary Figure 5D–F]. The IFNγ signalling pathway was completely inhibited using siRNA at 0.2, 1 or 10 nM final concentration [Supplementary Figure 5G to 5I], tofacitinib at 1 µM and filgotinib at 5 µM [Supplementary Figure 5J–L]. Therefore, we chose 10 nM as the final concentration for siRNA transfection, 1 µM of tofacitinib and 2 or 5 µM of filgotinib incubation for further studies on signalling cascades.

We showed that siHJ1D8 and siHJ1D2 transfection abolished IL22-induced STAT3 activation, IFNγ-induced STAT1 activation, IFNβ-induced STAT2 and STAT1 activation, as well as IL4-induced STAT3 and STAT1 activation in CACO-2 cells [Figure 3A–D]. To confirm these results obtained in CACO-2 cells, the same experiment was conducted in T47D and/or PC3 cells using IL22, IFNγ or IFNβ stimulation [Supplementary Figure 6A–C]. As expected, because JAK3 was not involved in these pathways, *JAK3*-targeting siHJ3D41 and siHMJ3D1 had no effect on IL22, IFNγ or IFNβ signalling, indicating perfect siRNA selectivity. Of note, tofacitinib and filgotinib also exerted an inhibitory effect but to a lesser extent for the latter. PC3 cells have also been stimulated by IL4 to analyse whether the other IL4 receptor isoform [IL4Rα and IL4Rγ_c] was involved in signal transduction through JAK1 and JAK3 in this cell line.[29–31] However, we observed that JAK3 was not involved in the IL4 response in CACO-2, PC3 nor T47D cells [respectively Figure 3D, and Supplementary Figure 6D and E]. To examine the efficacy of *JAK3*-targeting siRNA on JAK/STAT signalling, PC3 and T47D cells were stimulated by IL9. siHJ3D41 was the only one to exhibit a decrease in STAT1 phosphorylation [Supplementary Figure 6F and G]. Overall, using our siRNA approach, we showed that JAK1 seems to be the most important signalling hub for JAK/STAT-mediated signal transduction in these cell lines in the context of IL22, IFNγ, IFNβ and IL4 stimulation, but IL9 signalling seems to involve both *JAK1* and *JAK3*. In addition, we demonstrated that the *JAK1*- and *JAK3*-targeting siRNAs at 10 nM have a highly selective effect on JAK/STAT signalling and a similar, or an even superior, effect on IL22 and IFNγ, to a dose of 1 µM of tofacitinib or 5 µM of filgotinib.

lipofectamine RNAiMAX at 10 nM of siRNA or treatment by different concentrations of tofacitinib or filgotinib for 72 h. Cells were incubated with 5 µM EdU for 5 h, before harvesting and fixating the cells for downstream FACS analysis. Dot plot showing mean percentage ± SD [$N = 4$ independent experiments]; *p*-values: * = 0.0157, *** = 0.0010. [G] Analysis of apoptotic cell death in CACO-2 cells occurring after transfection by lipofectamine RNAiMAX at 10 nM of siRNAs or treated by different concentrations of tofacitinib or filgotinib, in the presence of 2 µM of CellEvent reagent for 72 h. Cells were harvested and fixated before downstream FACS analysis. Dot plot showing mean percentage ± SD [$N = 4$ independent experiments]; *p*-values: * = 0.0137 and 0.0204. [H] Mitochondrial metabolism and ATP levels were assessed in CACO-2 cells, following transfection by lipofectamine RNAiMAX at 10 nM of siRNAs or treated by different concentrations of tofacitinib or filgotinib for 72 h. Cells were then analysed using a ViaLight Plus Cell Proliferation and Cytotoxicity Bioassay kit. Dot plot showing mean percentage ± SD [$N = 4$ independent experiments]; *p*-values: * = 0.0143, ** = 0.0051.

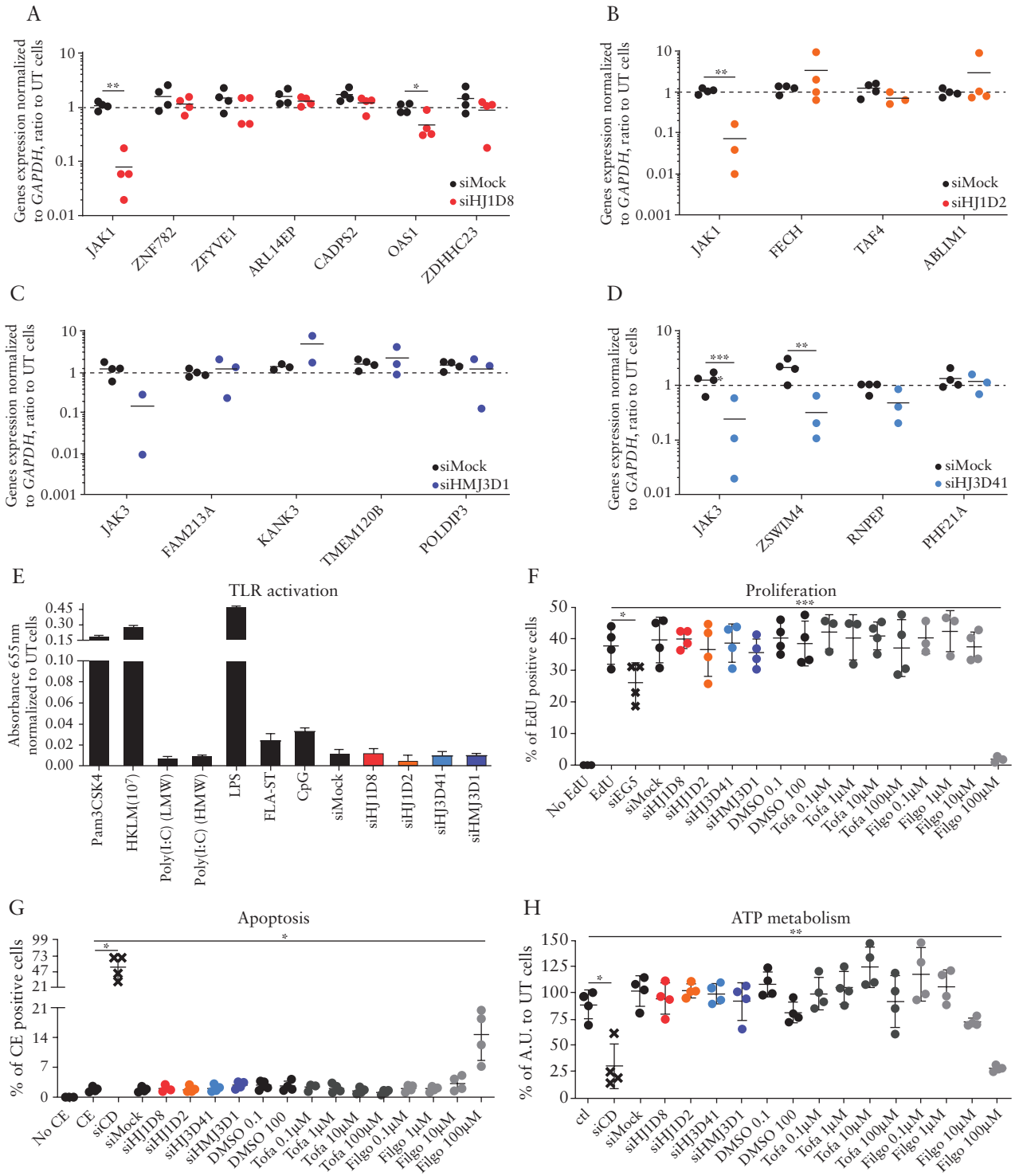

Figure 3. Comparative analysis of *JAK*-targeting siRNA and Jakinibs on JAK/STAT signalling in CACO-2 cells. Western blot analysis of JAK/STAT signalling in CACO-2 cells transfected at 10 nM siRNA using lipofectamine RNAiMAX for 48 h. Untransfected cells were then exposed to tofacitinib at 1 µM or filgotinib at 2 or 5 µM for 1 h. To trigger the activation of the JAK/STAT signalling pathway, cells were then exposed for 30 min to 10 ng/mL IL22 [A], IFNγ [B], IFNβ [C] or IL4 [D]. Quantification of at least $N = 4$ independent experiments, with each dot representing one '*N*', with means in black. *p*-values: * = <0.05, ** = 0.0079. Exact *p*-values are given in Supplementary Table 7.

3.6. *JAK*-targeting siRNAs do not lead to off-target effects at transcriptomic or proteomic levels

To verify the specificity of our *JAK*-targeting siRNAs, we performed unbiased broad-scale studies to analyse the potential off-target effects at both transcriptomic and proteomic levels. First, we conducted an RNASeq experiment to assess the transcriptomic profile of *JAK*-targeting siRNA-transfected cells and compared them to those of tofacitinib- or filgotinib-exposed cells in the absence of

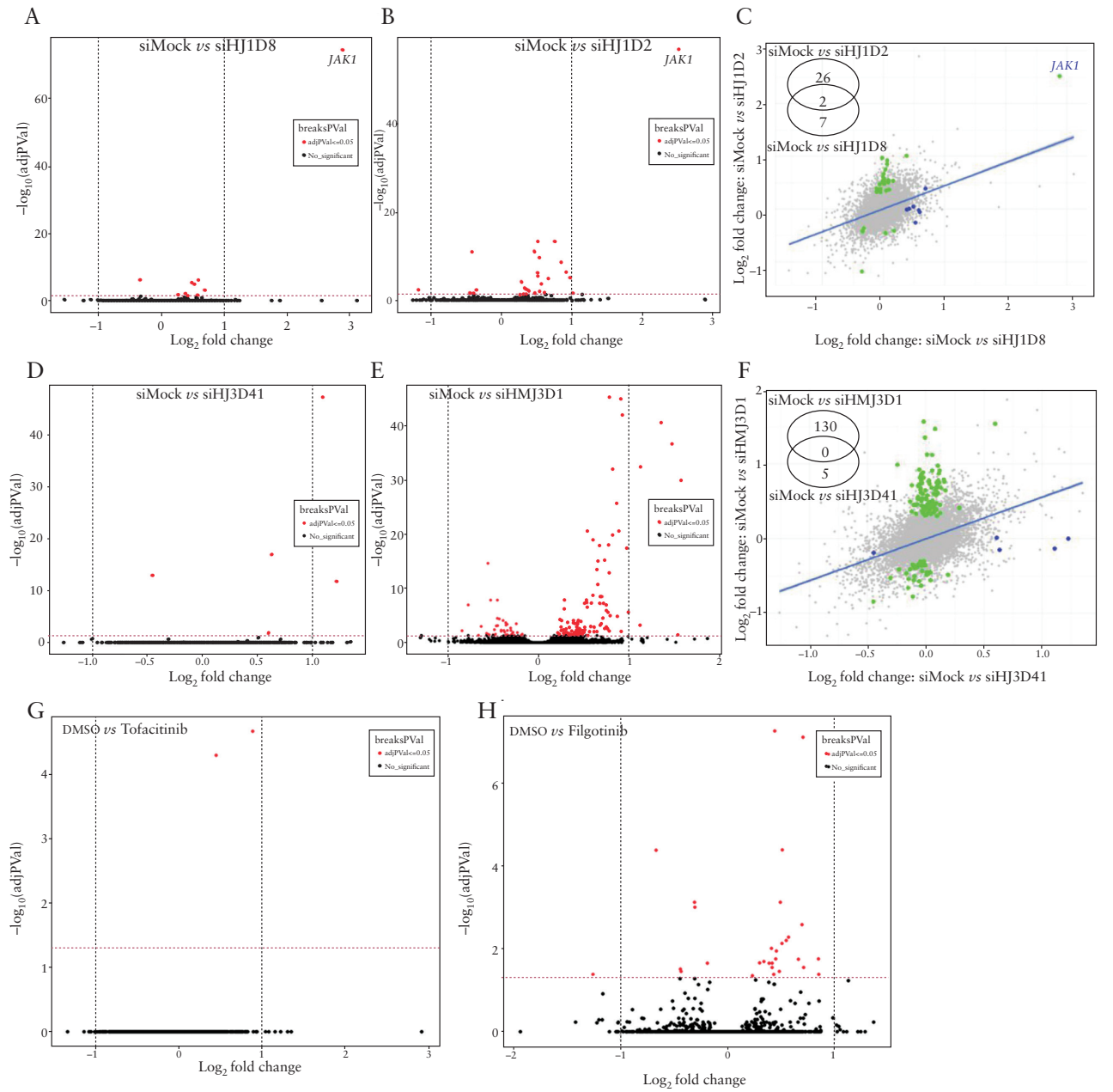

Figure 4. Omics analysis of off-target effects. [A–F] RNASeq analysis of CACO-2 cells transfected by 100 pM of *JAK*-targeting siRNAs or incubated with tofacitinib [1 μM] or filgotinib [2 μM] for 2 days. Volcano plot of differentially expressed genes [DEGs] of siHJ1D8 *vs* siMock conditions [A]; siHJ1D2 *vs* siMock conditions [B]. [C] Differential analysis of the DEGs obtained in A *vs* B with the corresponding Venn diagram. Volcano plot of DEGs of siHJ3D41 *vs* siMock conditions [D]; siHMJ3D1 *vs* siMock conditions [E]. [F] Differential analysis of the DEGs obtained in D *vs* E with the corresponding Venn diagram. Volcano plot of DEGs of tofacitinib *vs* DMSO conditions [G]; filgotinib *vs* DMSO conditions [H].

pro-inflammatory stimulations. To ensure a good JAK knockdown efficiency of the analysed samples, we confirmed the siRNA and Jakinibs efficacy at both protein and mRNA levels [using target genes] [Supplementary Figure 7A–C and D, respectively]. The analysis of differentially expressed genes [DEGs] between negative controls was also conducted and revealed very few off-target effects for DMSO *vs* cell medium conditions, as well as siMock *vs* transfection reagent alone conditions [Supplementary Figure 7E and F, respectively]. However, both transfection reagent and siMock [plus transfection reagent] *vs* cell medium conditions displayed higher DEGs, highlighting an impact of the transfection using lipofectamine RNAiMAX at the transcriptomic level [Supplementary Figure 7G and H, respectively]. The siMock *vs* siHJ1D8 and siHJ1D2 conditions showed nine and 28 DEGs, respectively [Figure 4A and B, respectively], with two in common between them [one of which is actually *JAK1*—Figure 4C]. The siMock *vs* siHJ3D41 and siHMJ3D1 conditions showed five and 130 DEGs, respectively [Figure 4D and E, respectively], but no common genes [Figure 4F]. DMSO *vs* tofacitinib and filgotinib showed two and 27 DEGs, respectively [Figure 4G and H, respectively]. Second, we analysed changes in protein expression using the SomaScan Proteomics platform developed by the SomaLogic Company. This proteomic

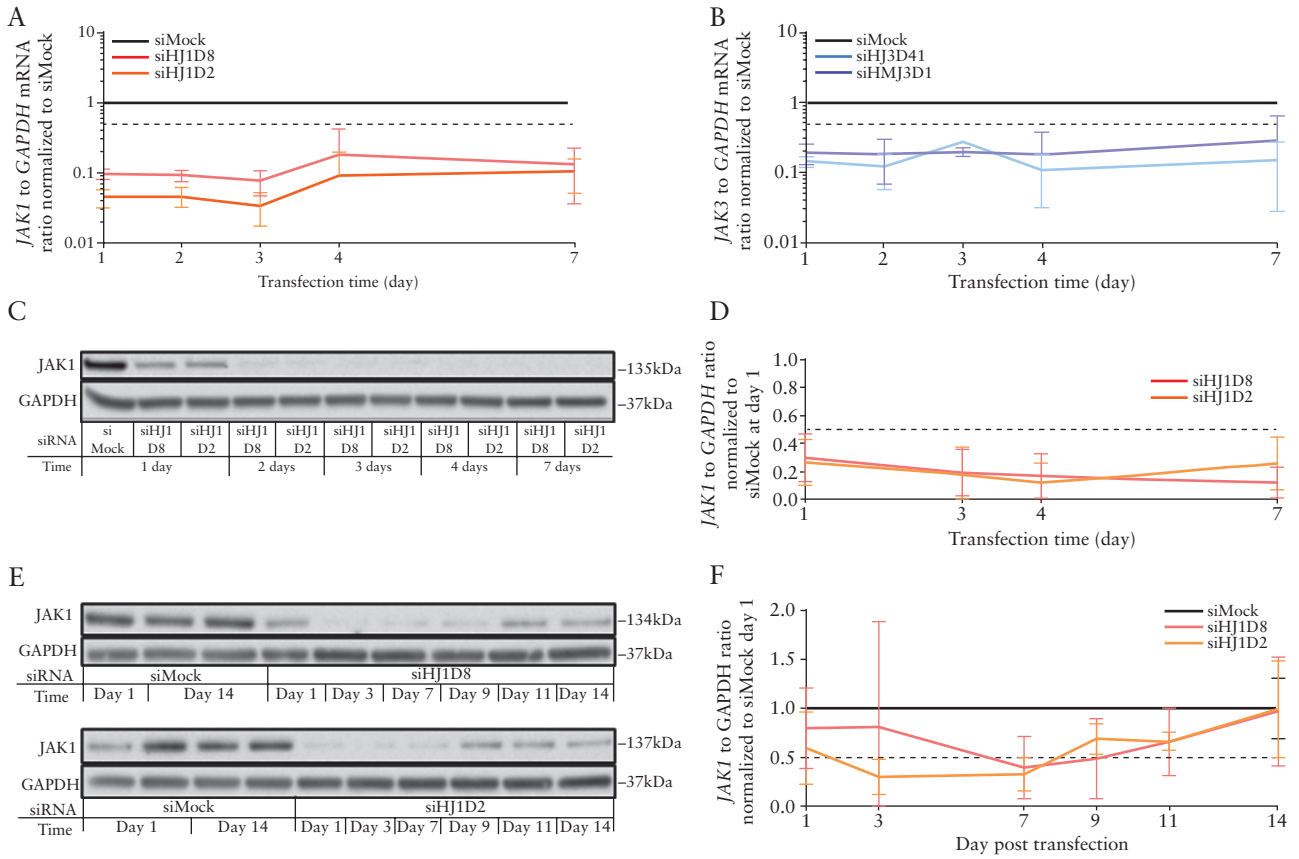

Figure 5. Efficiency of *JAK*-targeting siRNAs over time. RT-qPCR analysis of CACO-2 cells transfected by 10 nM siHJ1D8/2 with lipofectamine RNAiMAX for 1–7 days [*N* = 4 independent experiments, mean and SD represented] for the expression of *JAK1* [A] or *JAK3* [B]. Western-blot analysis of CACO-2 cells transfected by 10 nM siHJ1D8/2 with lipofectamine RNAiMAX for 1–7 days with a representative western blot analysis [C], and the corresponding quantification at the bottom [*N* = 6 independent experiments, mean and SD represented] for the expression of JAK1 [D]. Western blot analysis of CACO-2 cells pulse transfected for 6 h by 10 nM siHJ1D8/2 with lipofectamine RNAiMAX and analysed 1–14 days after transfection with a representative western blot analysis [E] and the corresponding quantification at the bottom [*N* = 3 independent experiments, mean and SD represented] for the expression of JAK1 [F].

approach allowed us to analyse the transfection effect of our siRNA sequences on the expression level of 1305 different proteins. To ensure the good quality of our samples, we verified JAK1 knockdown by western blotting, thereby confirming their quality in terms of transfection efficiency, with a strong knockdown of JAK1 induced by our siRNAs siHJ1D8 and siHJ1D2 [Supplementary Figure 7I]. The analysis of DEPs between *JAK*-targeting siRNAs and negative control showed 19, 39, 11 and 124 proteins that were differently expressed in siHJ1D8, siHJ1D2, siHJ3D41 and siHMJ3D1 conditions, respectively, with a fold change > 1.23 and a p-value < 0.05 [Supplementary Figure 8]. Together, these results highlighted a specificity profile of siHJ1D8, siHJ1D2 and siHJ3D41 compatible with further clinical applications. However, siHMJ3D1 presents a higher risk of off-target effects at both proteomic and transcriptomic levels. Of note, our data also demonstrated that the profile of transcriptomic changes induced by tofacitinib showed a better specificity for this drug than filgotinib.

3.7. Long-lasting effect of *JAK*-targeting siRNAs

To evaluate the clinical potential of using *JAK*-targeting siRNAs, we then analysed the kinetics of siRNA efficiency. We first assayed the minimal time for siRNA transfection by performing a 3–9 h transfection pulse. The data revealed a knockdown efficiency for both *JAK1* and *JAK3* after only 3 h of transfection at the mRNA level [respectively Supplementary Figure 9A and B], while at the protein level, their expression level was downregulated after 7 h [Supplementary Figure 9C]. The difference between protein and mRNA downregulation may be due to JAK proteins' half-life.[32] To assess the long-lasting effect of *JAK*-targeting siRNA transfection, we transfected CACO-2 cells and analysed JAK expression for 1–7 days. We confirmed that the siMock transfection did not affect JAK1 at the protein level [Supplementary Figure 9D]. The analysis of *JAK1* and *JAK3* at the transcriptomic level showed a complete silencing from Day 2 to Day 7 [respectively Figure 5A and B], which was confirmed at the protein level for JAK1 from Day 1 to Day 7 [Figure 5C and D]. Furthermore, we performed pulse transfection analysis over time, to ensure the long-term efficiency did not result from the siRNA remaining in the cell media. We first assayed 1, 3 and 6 h pulse transfection and analysed JAK expression 2 days post-transfection in order to choose the best pulse transfection timing. The data showed that complete JAK1 protein downregulation and STAT phosphorylation were observed with a 6 h pulse transfection [Supplementary Figure 9E]. We performed a 6 h transfection pulse of *JAK1*-targeting siRNA and monitored subsequent JAK1 expression for 14 days. Strikingly JAK1 downregulation was effective for 11 days [Figure 5E and F]. Our results thus showed a very interesting long-lasting efficiency of JAK downregulation even after a short pulse of siRNA transfection, further highlighting the clinical potential of RNAi to modulate the activity of JAK proteins.

4. Discussion

In the present study, we provided a framework using the DSIR program to design several siRNA sequences targeting *JAK1* or *JAK3*. We selected the two sequences displaying the lowest off-target effects while showing the highest efficiency at a concentration as low as 5 pM. As off-target effects are concentration-dependent, the possibility of using siRNAs at a very low concentration demonstrates the high potential of our siRNAs as drug candidates for therapeutic use.[24,33] The slight decrease of *TYK2* expression under *JAK1*-targeting siRNA transfection should be further evaluated for its presence in the majority of JAK1 membrane receptor complexes. Moreover, *TYK2* is also a target gene of Jakinibs in inflammatory bowel disease that may be another therapeutic agent for Crohn's disease.[34] Unbiased *in silico* and genome-wide omics approaches allowed us to ensure the specificity of the designed siRNAs. These approaches allowed us to propose three siRNA sequences with fewer than 40 off-target genes, at lower than the two-fold level that was a threshold assessed as acceptable by Birmingham and colleagues.[33] Combined with a phenotypic study of the *in cellulo* effect of our sequences, our data supported the potential for further clinical testing of three of the four selected sequences. Moreover, we provided a comparative analysis between *JAK*-targeting siRNAs and chemical inhibitors tofacitinib or filgotinib, with respect to their activity to modulate JAK/STAT signalling. Interestingly, we showed at least a ten-fold difference in efficacy between tofacitinib and filgotinib, which also corresponds to the doses administered to patients in clinical trials [respectively 10–20 mg daily *vs* 200 mg daily].[35,36] These Jakinibs chemical inhibitors were shown to exhibit dramatic side-effects, including infections, and haematological and cardiovascular effects mainly due to unspecific JAK targeting that could be avoided using *JAK1*- or *JAK3*-specific siRNAs.[11,37]

For instance, in 2019, Salguero-Aranda and colleagues developed a *STAT6*-targeting siRNA for treatment of cancer. Their optimal siRNA concentrations to knockdown STAT6 at the protein level [at least 60% inhibition] *in vitro* were 100 nM in HT-29 colorectal cancer cells and ZR-75-1 breast cancer cells, which are much higher compared to the 10 pM concentration of the *JAK*-targeting siRNAs described in this study. Moreover, they showed an effect lasting 7 days post-transfection,[38] while we were able to observe a knockdown of JAK1 at the protein level even 11 days after a 6-h pulse. This long-term efficacy at ultra-low doses would make it possible to consider a protocol for patients with low constraints, thus improving their quality of life.

Until now, siRNA therapeutics have been poorly investigated in the context of inflammatory bowel diseases. A chemically modified antisense oligonucleotide targeting SMAD7, an intracellular protein that blocks TGFβ signalling, has been investigated in clinical trials for patients with Crohn's disease.[39] TGFβ is a cytokine which negatively regulates inflammation, and its defective activity can lead to the development of colitis. Interestingly, SMAD7 inhibition restores TGFβ signaling and activity, thus leading to decreased production of inflammatory cytokines. In this study, the antisense oligonucleotide is embedded as 'naked' in an external tablet coating made of pH-sensitive polymers used for oral delivery purposes. Unfortunately, the subsequent phase III trial was terminated early because of a lack of efficacy.[40] In animal models of experimental colitis, other targets have been considered for inhibition through siRNAs, such as TNFα[41,42] or CD98,[43] leading to slight improvements in body weight recovery after colitis induction. In these studies, the siRNA was delivered through different polymer particles, using either polyethylenimine [PEI][42,43] or synthetic polymers smartly designed to be sensitive to environmental factors.[41] These studies suffer from several limitations with regard to future product development in the field using siRNA therapeutics: [i] their targets do not lead to a broader inhibition of inflammation, in contrast to JAK inhibition that interferes with several signalling cascades of pro-inflammatory mediators, and [ii] their delivery systems are either complicated and costly to consider for scaled up production or present some toxicity issues. In this context, the design of siRNA therapeutics leading to a broad inhibition of mucosal inflammation is still highly anticipated and associated with challenges with regard to local delivery. For instance, lipid nanoparticles are widely used *in vivo* to deliver RNA, and some products are even already on the market, such as Onpattro or COVID-19 vaccines.[16,44,45] However, the delivery challenge to reach some immune cells in the lamina propria of intestines is especially high as the carrier has to overcome several biological obstacles, such as stability in the colonic lumen and its harsh environment, transport across the mucus layer and the underlying epithelial barrier and finally transfection across the plasma membrane of the target cells. No carrier has previously been available on the market or in R&D with high maturity level that fulfils all the aforementioned criteria. Lipid nanoparticles are interesting, but Ball and colleagues have demonstrated that intestinal fluids could trigger their aggregation, thus hampering their potency.[46] Moreover, these lipid particles cannot easily diffuse through the mucus layer. Intensive research is still needed to design and validate the most appropriate carrier for the local delivery of RNA in the inflamed gut, with good control on their toxicity and feasibility for scaled up production at reasonable costs. Indeed, a recent review by Saw and Song,[47] highlighting the potential of siRNA therapeutics, underlined the benefits of siRNAs as compared to small-molecule drugs, including specificity, potency, high selectivity with low toxicity, and stable serum stability. The authors raised the issue that it is the route of administration such as electroporation, local injection or topical application [mucosa, oral or rectal] that remains the biggest challenge of siRNA therapeutics, not the development of potent and safe siRNA.[47] Addressing delivery issues would lead towards a targeted medicine at several levels—molecular through the RNAi and cellular and tissular through specific vectorization.

Future work should emphasize testing the *in vivo* stability of our *JAK*-targeting siRNAs, as well as their *in vivo* efficiency, either in human 3D organoids or in biopsies rather than animal models, as the sequence specificity of our siRNA-designed sequences restricted their use in human cellular models. In addition, many cases reported that animal models with mice or rodents often do not accurately recapitulate human inflammatory diseases.[48] In this regard, the recent development of siRNA transfection in 3D should improve the preclinical testing of therapeutic siRNAs.[49] Developing new therapeutics highly specific to either *JAK1* or *JAK3* could be greatly beneficial for patients with cancer and immune-related diseases, or even infections. Indeed, JAK1 and JAK3 have been widely described as potential therapeutic targets for several types of cancer, including gliomas,[50,51] head and neck cancers and oesophageal squamous cell carcinoma,[52,53,54,55] breast cancer,[56,57] multiple myeloma,[58,59] colon cancer[60,61] and pancreatic cancer,[62–64] as well as for developing cancer immunotherapies.[65] JAK3 has been particularly highlighted as a therapeutic target in immune cell-related cancers, including B-lineage acute lymphoblastic leukaemia[66] and natural killer/T-cell lymphoma,[67] and also for improving allotransplantation.[68,69] Both *JAK1* and *JAK3* selective downregulation could also be of great benefit for inflammatory bowel disease patients,[70] and autoimmune and inflammatory disease-related patients.[6,71] Targeting the JAK/STAT pathway would also benefit patients with diseases related to JAK1 or JAK3 overactivation, including COVID-19 patients. Indeed,

the use of Jakinibs has been recently suggested to treat Covid-19 patients, for instance ruxolitinib for the treatment COVID-19-related cytokine storm,[72] or barcitinib, which also displayed promising outcomes even in elderly patients.[73]

In conclusion, we have provided a detailed analysis of both the specificity profile and efficacy of new *JAK1*- and *JAK3*-targeting siRNAs. We hope our work will pave the way for novel therapeutics exploiting RNAi in inflammatory diseases.

Funding

This research was funded by the European Union's Horizon 2020 research and innovation programme H2020 'NEWDEAL' [grant agreement No. 720905]. F.C., A.N. and A.D. were supported by a fellowship from the H2020 NEWDEAL project. This publication reflects only the authors' views, and the Commission is not responsible for any use that may be made of the information it contains. This project received funding from CEA and GRAL, a programme from the Chemistry Biology Health [CBH] Graduate School of University Grenoble Alpes [ANR-17-EURE-0003].

Conflict of Interest

The authors have declared that no conflict of interest exists. The world patent WO2021009126 [A1] covers the use of siRNA sequences targeting the expression of human genes JAK1 or JAK3 for therapeutic use.

Author Contributions

X.G. conceived the study. F.C., E.S., A.K.D., F.P.B., P.N.M. and X.G. designed research studies. F.C., A.N., S.C., F.K., A.K.D., P.O., A.M. and E.S. conducted experiments, and acquired and analysed data. F.P.N., A.M., P.N.M. and X.G. provided reagents. F.C., A.N. and X.G. wrote the manuscript. All authors provided final approval for this manuscript to be published.

Data Availability Statement

The data underlying this article were generated from the IPMC platform [Nice, France] and SomaLogic company [Boulder, CO, USA]. The data underlying this article are available in the ArrayExpress database [fgsubs #491636] and will be shared on reasonable request to the corresponding author.

Acknowledgements

We gratefully acknowledge financial support by the European Union's Horizon 2020 research and innovation programme H2020 'NEWDEAL' [grant agreement No. 720905]. We also would like to thank Scienseed company for designing the graphical abstract.

Supplementary Data

Supplementary data are available at *ECCO-JCC* online.

References

1. David T, Ling SF, Barton A. Genetics of immune-mediated inflammatory diseases. *Clin Exp Immunol* 2018;**193**:3–12.
2. Kahn J, Deverapalli SC, Rosmarin D. JAK-STAT signaling pathway inhibition: a role for treatment of various dermatologic diseases. *Semin Cutan Med Surg* 2018;**37**:198–208.
3. Luo W, Li Y-X, Jiang L-J, Chen Q, Wang T, Ye D-W. Targeting JAK-STAT signaling to control cytokine release syndrome in COVID-19. *Trends Pharmacol Sci*. Published online June 17, 2020. doi:10.1016/j.tips.2020.06.007
4. Murray PJ. The JAK-STAT signaling pathway: input and output integration. *J Immunol* 2007;**178**:2623–9.
5. Takahashi T, Fukuda K, Pan J, *et al*. Characterization of insulin-like growth factor-1-induced activation of the JAK/STAT pathway in rat cardiomyocytes. *Circ Res* 1999;**85**:884–91.
6. Clark JD, Flanagan ME, Telliez JB. Discovery and development of Janus kinase (JAK) inhibitors for inflammatory diseases. *J Med Chem* 2014;**57**:5023–38.
7. Hernandez-Rocha C, Vande Casteele N. JAK inhibitors: current position in treatment strategies for use in inflammatory bowel disease. *Curr Opin Pharmacol* 2020;**55**:99–109.
8. Sandborn WJ, Peyrin-Biroulet L, Quirk D, *et al*. Efficacy and safety of extended induction with tofacitinib for the treatment of ulcerative colitis. *Clin Gastroenterol Hepatol*. Published online October 27, 2020. doi:10.1016/j.cgh.2020.10.038
9. Dhillon S, Keam SJ. Filgotinib: first approval. *Drugs* 2020;**80**:1987–97.
10. Galapagos NV. *Double-blind, randomized, placebo-controlled, multicentre study to investigate the efficacy and safety of GLPG0634 in subjects with active Crohn's disease with evidence of mucosal ulceration*. clinicaltrials.gov; 2016. https://clinicaltrials.gov/ct2/show/NCT02048618
11. Gadina M, Le MT, Schwartz DM, *et al*. Janus kinases to jakinibs: from basic insights to clinical practice. *Rheumatology (Oxford)* 2019;**58**:i4–i16.
12. Ma C, Jairath V, Vande Casteele N. Pharmacology, efficacy and safety of JAK inhibitors in Crohn's disease. *Best Pract Res Clin Gastroenterol* 2019;**38-39**:101606.
13. Colombel J-F, Osterman MT, Thorpe AJ, *et al*. Maintenance of remission with tofacitinib therapy in patients with ulcerative colitis. *Clin Gastroenterol Hepatol*. Published online October 9, 2020. doi:10.1016/j.cgh.2020.10.004
14. Fire A, Xu S, Montgomery MK, Kostas SA, Driver SE, Mello CC. Potent and specific genetic interference by double-stranded RNA in *Caenorhabditis elegans*. *Nature* 1998;**391**:806–11.
15. Setten RL, Rossi JJ, Han SP. The current state and future directions of RNAi-based therapeutics. *Nat Rev Drug Discov* 2019;**18**:421–46.
16. Adams D, Gonzalez-Duarte A, O'Riordan WD, *et al*. Patisiran, an RNAi therapeutic, for hereditary transthyretin amyloidosis. *N Engl J Med* 2018;**379**:11–21.
17. Second RNAi drug approved. *Nat Biotechnol* 2020;**38**:385. doi:10.1038/s41587-020-0494-3
18. Jackson AL, Linsley PS. Recognizing and avoiding siRNA off-target effects for target identification and therapeutic application. *Nat Rev Drug Discov* 2010;**9**:57–67.
19. Court M, Malier M, Millet A. 3D type I collagen environment leads up to a reassessment of the classification of human macrophage polarizations. *Biomaterials* 2019;**208**:98–109.
20. Vert JP, Foveau N, Lajaunie C, Vandenbrouck Y. An accurate and interpretable model for siRNA efficacy prediction. *BMC Bioinformatics* 2006;**7**:520.
21. Matveeva O. What parameters to consider and which software tools to use for target selection and molecular design of small interfering RNAs. *Methods Mol Biol* 2013;**942**:1–16.
22. Li C, Zamore PD. RNA interference and small RNA analysis. *Cold Spring Harb Protoc* 2019;**2019**:pdb.top097436.
23. Jackson AL, Bartz SR, Schelter J, *et al*. Expression profiling reveals off-target gene regulation by RNAi. *Nat Biotechnol* 2003;**21**:635–7.
24. Jackson AL, Burchard J, Schelter J, *et al*. Widespread siRNA "off-target" transcript silencing mediated by seed region sequence complementarity. *RNA* 2006;**12**:1179–87.
25. Burchard J, Jackson AL, Malkov V, *et al*. MicroRNA-like off-target transcript regulation by siRNAs is species specific. *RNA* 2009;**15**:308–15.
26. Matveeva O, Nechipurenko Y, Rossi L, *et al*. Comparison of approaches for rational siRNA design leading to a new efficient and transparent method. *Nucleic Acids Res* 2007;**35**:e63.
27. Mroweh M, Decaens T, Marche PN, Macek Jilkova Z, Clément F. Modulating the crosstalk between the tumor and its microenvironment using RNA interference: a treatment strategy for hepatocellular carcinoma. *Int J Mol Sci* 2020;**21**:5250.
28. Nejepinska J, Flemr M, Svoboda P. Control of the interferon response in RNAi experiments. *Methods Mol Biol* 2012;**820**:133–61.

29. Umeshita-Suyama R, Sugimoto R, Akaiwa M, *et al*. Characterization of IL-4 and IL-13 signals dependent on the human IL-13 receptor alpha chain 1: redundancy of requirement of tyrosine residue for STAT3 activation. *Int Immunol* 2000;**12**:1499–509.
30. Busch-Dienstfertig M, González-Rodríguez S. IL-4, JAK-STAT signaling, and pain. *JAKSTAT* 2013;**2**:e27638.
31. Chang TL, Peng X, Fu XY. Interleukin-4 mediates cell growth inhibition through activation of Stat1. *J Biol Chem* 2000;**275**:10212–7.
32. Siewert E, Müller-Esterl W, Starr R, Heinrich PC, Schaper F. Different protein turnover of interleukin-6-type cytokine signalling components. *Eur J Biochem* 1999;**265**:251–7.
33. Birmingham A, Anderson E, Sullivan K, *et al*. A protocol for designing siRNAs with high functionality and specificity. *Nat Protoc* 2007;**2**:2068–78.
34. Rogler G. Efficacy of JAK inhibitors in Crohn's Disease. *J Crohns Colitis* 2020;**14**:746–54.
35. Pfizer. *A multi-center, open-label study of CP-690,550 in subjects with moderate to severe ulcerative colitis*. clinicaltrials.gov; 2021. https://clinicaltrials.gov/ct2/show/study/NCT01470612
36. Gilead Sciences. *A multicenter, open-label, long-term follow-up safety and efficacy study of GLPG0634 treatment in subjects with moderately to severely active rheumatoid arthritis*. clinicaltrials.gov; 2021. https://clinicaltrials.gov/ct2/show/NCT02065700
37. Gadina M, Johnson C, Schwartz D, *et al*. Translational and clinical advances in JAK-STAT biology: the present and future of jakinibs. *J Leukoc Biol* 2018;**104**:499–514.
38. Salguero-Aranda C, Sancho-Mensat D, Canals-Lorente B, Sultan S, Reginald A, Chapman L. STAT6 knockdown using multiple siRNA sequences inhibits proliferation and induces apoptosis of human colorectal and breast cancer cell lines. *PLoS One* 2019;**14**:e0207558.
39. Monteleone G, Pallone F. Mongersen, an oral SMAD7 antisense oligonucleotide, and Crohn's disease. *N Engl J Med* 2015;**372**:2461.
40. Bewtra M, Lichtenstein GR. Mongersen and SMAD-7 inhibition, not a lucky 7 for patients with IBD: when trial design is as important as disease therapy. *Am J Gastroenterol* 2020;**115**:687–8.
41. Wilson DS, Dalmasso G, Wang L, Sitaraman SV, Merlin D, Murthy N. Orally delivered thioketal nanoparticles loaded with TNF-α-siRNA target inflammation and inhibit gene expression in the intestines. *Nat Mater* 2010;**9**:923–8.
42. Frede A, Neuhaus B, Klopfleisch R, *et al*. Colonic gene silencing using siRNA-loaded calcium phosphate/PLGA nanoparticles ameliorates intestinal inflammation in vivo. *J Control Release* 2016;**222**:86–96.
43. Laroui H, Geem D, Xiao B, *et al*. Targeting intestinal inflammation with CD98 siRNA/PEI-loaded nanoparticles. *Mol Ther* 2014;**22**:69–80.
44. Polack FP, Thomas SJ, Kitchin N, *et al*.; C4591001 Clinical Trial Group. Safety and efficacy of the BNT162b2 mRNA Covid-19 vaccine. *N Engl J Med* 2020;**383**:2603–15.
45. Baden LR, El Sahly HM, Essink B, *et al*. Efficacy and safety of the mRNA-1273 SARS-CoV-2 vaccine. *N Engl J Med*. Published online December 30, 2020:NEJMoa2035389. doi:10.1056/NEJMoa2035389
46. Ball RL, Bajaj P, Whitehead KA. Oral delivery of siRNA lipid nanoparticles: fate in the GI tract. *Sci Rep* 2018;**8**:2178.
47. Saw PE, Song EW. siRNA therapeutics: a clinical reality. *Sci China Life Sci* 2020;**63**:485–500.
48. Seok J, Warren HS, Cuenca AG, *et al*.; Inflammation and Host Response to Injury, Large Scale Collaborative Research Program. Genomic responses in mouse models poorly mimic human inflammatory diseases. *Proc Natl Acad Sci U S A* 2013;**110**:3507–12.
49. Laperrousaz B, Porte S, Gerbaud S, *et al*. Direct transfection of clonal organoids in Matrigel microbeads: a promising approach toward organoid-based genetic screens. *Nucleic Acids Res* 2018;**46**:e70.
50. Rajappa P, Cobb WS, Vartanian E, *et al*. Malignant astrocytic tumor progression potentiated by JAK-mediated recruitment of myeloid cells. *Clin Cancer Res* 2017;**23**:3109–19.
51. Wei J, Ma L, Li C, Pierson CR, Finlay JL, Lin J. Targeting upstream kinases of STAT3 in human medulloblastoma cells. *Curr Cancer Drug Targets* 2019;**19**:571–82.
52. Vakili Saatloo M, Aghbali AA, Koohsoltani M, Yari Khosroushahi A. Akt1 and Jak1 siRNA based silencing effects on the proliferation and apoptosis in head and neck squamous cell carcinoma. *Gene* 2019;**714**:143997.
53. Zhang Z, Liu F, Li Z, Wang D, Li R, Sun C. Jak3 is involved in CCR7-dependent migration and invasion in metastatic squamous cell carcinoma of the head and neck. *Oncol Lett* 2017;**13**:3191–7.
54. You Z, Xu D, Ji J, Guo W, Zhu W, He J. JAK/STAT signal pathway activation promotes progression and survival of human oesophageal squamous cell carcinoma. *Clin Transl Oncol* 2012;**14**:143–9.
55. Meng L, Wang F, Sun S, *et al*. MicroRNA-30b targets CBX3 and regulates cell proliferation, apoptosis, and migration in esophageal squamous cell carcinoma via the JAK2/STAT3 signaling pathway. *Int J Clin Exp Pathol* 2017;**10**:11828–37.
56. Wehde BL, Rädler PD, Shrestha H, Johnson SJ, Triplett AA, Wagner KU. Janus kinase 1 plays a critical role in mammary cancer progression. *Cell Rep* 2018;**25**:2192–2207.e5.
57. Henkels KM, Farkaly T, Mahankali M, Segall JE, Gomez-Cambronero J. Cell invasion of highly metastatic MTLn3 cancer cells is dependent on phospholipase D2 (PLD2) and Janus kinase 3 (JAK3). *J Mol Biol* 2011;**408**:850–62.
58. de Oliveira MB, Fook-Alves VL, Eugenio AIP, *et al*. Anti-myeloma effects of ruxolitinib combined with bortezomib and lenalidomide: a rationale for JAK/STAT pathway inhibition in myeloma patients. *Cancer Lett* 2017;**403**:206–15.
59. Kimura S. AT-9283, a small-molecule multi-targeted kinase inhibitor for the potential treatment of cancer. *Curr Opin Investig Drugs* 2010;**11**:1442–9.
60. Tang S, Yuan X, Song J, Chen Y, Tan X, Li Q. Association analyses of the JAK/STAT signaling pathway with the progression and prognosis of colon cancer. *Oncol Lett* 2019;**17**:159–64.
61. Lin Q, Lai R, Chirieac LR, *et al*. Constitutive activation of JAK3/STAT3 in colon carcinoma tumors and cell lines: inhibition of JAK3/STAT3 signaling induces apoptosis and cell cycle arrest of colon carcinoma cells. *Am J Pathol* 2005;**167**:969–80.
62. Liu Q, Guo L, Zhang S, Wang J, Lin X, Gao F. PRSS1 mutation: a possible pathomechanism of pancreatic carcinogenesis and pancreatic cancer. *Mol Med* 2019;**25**:44.
63. Smigiel JM, Parameswaran N, Jackson MW. Potent EMT and CSC phenotypes are induced by oncostatin-M in pancreatic cancer. *Mol Cancer Res* 2017;**15**:478–88.
64. Lu D, Qin Q, Lei R, Hu B, Qin S. Targeted blockade of interleukin 9 inhibits tumor growth in murine model of pancreatic cancer. *Adv Clin Exp Med* 2019;**28**:1285–92.
65. Chan LC, Li CW, Xia W, *et al*. IL-6/JAK1 pathway drives PD-L1 Y112 phosphorylation to promote cancer immune evasion. *J Clin Invest* 2019;**129**:3324–38.
66. Uckun FM, Pitt J, Qazi S. JAK3 pathway is constitutively active in B-lineage acute lymphoblastic leukemia. *Expert Rev Anticancer Ther* 2011;**11**:37–48.
67. Nairismägi M-, Gerritsen ME, Li ZM, *et al*. Oncogenic activation of JAK3-STAT signaling confers clinical sensitivity to PRN371, a novel selective and potent JAK3 inhibitor, in natural killer/T-cell lymphoma. *Leukemia* 2018;**32**:1147–56.
68. Vassilev AO, Tibbles HE, DuMez D, Venkatachalam TK, Uckun FM. Targeting JAK3 and BTK tyrosine kinases with rationally-designed inhibitors. *Curr Drug Targets* 2006;**7**:327–43.
69. Kim JM, Shin JS, Min BH, *et al*. JAK3 inhibitor-based immunosuppression in allogeneic islet transplantation in cynomolgus monkeys. *Islets* 2019;**11**:119–28.
70. Coskun M, Salem M, Pedersen J, Nielsen OH. Involvement of JAK/STAT signaling in the pathogenesis of inflammatory bowel disease. *Pharmacol Res* 2013;**76**:1–8.
71. Banerjee S, Biehl A, Gadina M, Hasni S, Schwartz DM. JAK-STAT signaling as a target for inflammatory and autoimmune diseases: current and future prospects. *Drugs* 2017;**77**:521–46.
72. Goker Bagca B, Biray Avci C. The potential of JAK/STAT pathway inhibition by ruxolitinib in the treatment of COVID-19. *Cytokine Growth Factor Rev* 2020;**54**:51–62.
73. Stebbing J, Sánchez Nievas G, Falcone M, *et al*. JAK inhibition reduces SARS-CoV-2 liver infectivity and modulates inflammatory responses to reduce morbidity and mortality. *Sci Adv* 2021;**7**:eabe4724. doi:10.1126/sciadv.abe4724